International Journal of Control, Automation and Systems 15(5) (2017) 2364-2375
http://dx.doi.org/10.1007/s12555-016-0248-7
ISSN:1598-6446 eISSN:2005-4092
http://www.springer.com/12555

Torque Sensorless Force/position Decentralized Control for Constrained Reconfigurable Manipulator with Harmonic Drive Transmission

Fan Zhou, Bo Dong, and Yuanchun Li*

Abstract: The difficulty of addressing the decentralized control problem for a torque sensorless constrained reconfigurable manipulator is associated with decentralized control of the constraint force. This paper studies the force/position decentralized robust control problem for constrained reconfigurable manipulator system with parameter perturbation and unmodeled dynamics. A joint torque estimation scheme based on the motor-side and link-side position measurements along with harmonic drive model is deployed for each joint module. Subsequently, radial basis function (RBF) neural network is applied to compensate the unmodeled dynamics and unknown terms of subsystem, simultaneously. Furthermore, a decentralized force/position robust controller is designed by combining the estimated joint torque with the dynamic output feedback control method. The stability of closed-loop system is proved using the Lyapunov theory and linear matrix inequality (LMI) technique. Finally, simulations are performed to verify the advantage of the proposed method.

Keywords: Constrained reconfigurable manipulator, dynamic output feedback, force/position decentralized control, harmonic drive, linear matrix inequality (LMI).

1. INTRODUCTION

Since the first industrial reconfigurable manipulator was designed and developed by Schmitz *et al*. [1] from Carnegie Mellon University in the 1988, the robot designers and industrial manufacturers have devoted a considerable attention on developing reconfigurable manipulator. Through the untiring efforts of scholars, the research results for reconfigurable manipulators have been relatively mature. However, most of the existing researches for reconfigurable manipulator are carried out under the space which was totally free of environment constraints [2–5]. Actually, in most of practical applications such as polishing, grinding, crawling, assembling etc., the manipulator may inevitably contact the environments or manipulating objects [6–9]. Hence, it can hardly meet the application demands by simply controlling the position of manipulator.

In recent literatures, some researchers have paid much attention on controlling constrained manipulators. Bellakehal *et al*. [10] designed a force and position control for parallel kinematic machines. The originality of the approach resides in the use of a vision system as an exteroceptive pose measurement of a parallel machine tool for force control purposes. Karayiannidis and Doulgeri [11] deployed the problem of controlling robot motion and force in frictional contacts under environmental errors and particularly orientation errors that distort the desired control targets and control subspaces. Truong and Ahn [12] offered an online smart tuning fuzzy PID (OSTF-PID) approach based on a robust extended Kalman filter (REKF) for the development of high force control precision in the press machines. Hamid [13] concerned with the tracking control problem of robotic systems perturbed by time-varying parameters, unmodelled dynamics and external force (and moment) disturbances. However, the aforementioned methods were concentrated on centralized control. For practical purposes, a centralized controller designed on the basis of an entire system may not be applicable for reconfigurable manipulators system due to the high computation costs, robustness, and complexities. Compared with centralized control, decentralized control scheme can effectively reduce the computational burden of centralized control structure, so it is a well-known valid

Manuscript received April 22, 2016; revised October 23, 2016 and December 29, 2016; accepted January 26, 2017. Recommended by Associate Editor Sukho Park under the direction of Editor Hyun-Seok Yang. This work was supported by the National Natural Science Foundation of China (61374051 and 60974010) and Scientific and Technological Development Plan Project in Jilin Province of China (20160414033GH and 20160520013JH).

Fan Zhou is with Department of Control Science and Engineering, Changchun University of Technology, Changchun, China (e-mail: zhoufandyouxiang@sina.com). Bo Dong is with State Key Laboratory of Management and Control for Complex Systems, Institute of Automation, Chinese Academy of Sciences, Beijing, China. He is also with Department of Control Science and Engineering, Changchun University of Technology, Changchun, China (e-mail: dongbo@ccut.edu.cn). Yuanchun Li is with Department of Control Science and Engineering, Changchun University of Technology, Changchun, China. He is also with Department of Control Science and Engineering, Jilin University, Changchun, China (e-mail: liyc@ccut.edu.cn).
* Corresponding author.

control approach for reconfigurable manipulators. It should be stressed that, how to obtain each joint torque of constrained reconfigurable manipulator is a crucial issue for the purpose of achieving force decentralized control. Several techniques of direct joint torque sensing are proposed in the literatures [14–16]. But, using joint torque sensor measurements directly is known with many drawbacks and may spoil the reliability, ruggedness and simplicity of robot manipulators. Furthermore, most robot manipulators are not equipped with joint torque sensor, and it is difficult to add them due to mechanical design constraints. This paper proposes a novel decentralized force/position control method for constrained reconfigurable manipulators with harmonic drive transmission by estimating the joint torques with only position measurements.

Feedback control is predominantly considered as an effective technique for improving the performance of controller [17–20]. Due to the states of system are not always available in practical situations, the output feedback control method is developed. Compared with the state feedback control, the output feedback control problem is more challenging because of the limited information of state variables. The output feedback can be classified into two categories: static output feedback and dynamic output feedback. It is well known that the static output feedback is easy for implementation, but some strict conditions should be imposed on the system. The dynamic output feedback technique is more flexible and the required conditions on the considered systems are less conservative. Zhang *et al*. [21] presented a discrete event-triggering mechanism to determine whether or not a sampled signal packet will be transmitted for dynamic output feedback controller design. Wang *et al*. [22] introduced a dynamic output feedback controller for continuous-time NCSs considering packet dropouts and network-induced delays in the S-C channel, and network-induced delays in the C-A channel. Sami and Patton [23] described a novel fault tolerant tracking control (FTTC) strategy based on robust fault estimation and compensation of simultaneous actuator and sensor faults. However, these schemes worked under the condition that the dynamic model of control system is accurate. It is well known that the parameter perturbation and unmodeled dynamics are unavoidable in the reconfigurable manipulator system. Therefore, an excellent control method for constrained reconfigurable manipulator with parameter perturbation and unmodeled dynamics should be able to have high robustness. Although decentralized adaptive controllers can compensate for partially unknown manipulator dynamics, they often suffer from incapacity to deal with unstructured uncertainties [24–26]. Hence, it is necessary to develop the model-free adaptive control strategies. Recently, RBF neural networks are applied to identification analysis and design of control systems with satisfactory results. Jin *et al*. [27] implemented position control of a mobile inverted pendulum (MIP) system by using the radial basis function (RBF) network. Yu *et al*. [28] designed a review on different approaches of designing and training RBF networks and proved the RBF networks have advantages of easy design, good generalization, strong tolerance to input noise, and online learning ability. Golbabai and Rabiei [29] reviewed the available strategies in the literature for selecting shape parameters and introduced an alternative approach called hybrid strategy for scaling the RBFs. The major advantages in the RBF-based control schemes are that the developed controllers can be employed to deal with increasingly complex systems, to avoid the computation of the complicated regressor matrix, and to implement the controller without any precise knowledge of the structure of the entire dynamic model.

In this work, a torque sensorless force/position decentralized robust control method is presented for constrained reconfigurable manipulator. The unmodeled dynamics and unknown terms of subsystem are compensated by radial basis function (RBF) neural network. In addition, a novel joint torque estimation scheme that exploits the existing structural elasticity of manipulator joint with harmonic drive transmission is applied for each joint module and the decentralized robust dynamic output feedback controller is designed to realize the force/position control for constrained reconfigurable manipulator. Based on the Lyapunov theory, the sufficient condition for ensures the reconfigurable manipulator system asymptotically stable while satisfying a prescribed H_∞ performance level is offered in terms of linear matrix inequality (LMI). The main features of the proposed approach are: (i) it extends the position tracking control to position/force tracking control, which adapts to the increasing demands of reconfigurable manipulator contact to task environments and (ii) in comparison with existing results where only location decentralized control for reconfigurable manipulators was investigated, this paper presents a constrained force decentralized control method that is critical in real-time application.

The rest of this paper is organized as follows: In Section 2, the theory of harmonic drive transmission is introduced. In addition, the torque estimation algorithm is formulated. In Section 3, the nonlinear interconnected subsystem dynamic model of constrained reconfigurable manipulators is described. In Section 4, the main technical results of this paper are given, which include the neural network identification and the designs of robust controller. In Section 5, numerical simulation is performed to show the feasibility of the proposed approach. Finally, Section 6 draws the conclusion.

2. JOINT TORQUE ESTIMATION

Harmonic drives consist of three main components as

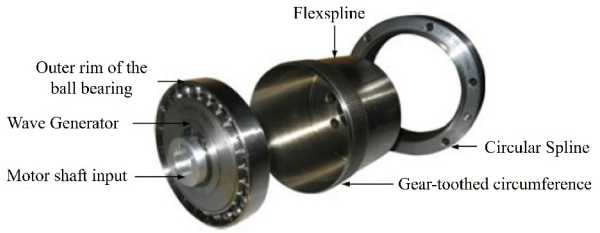

Fig. 1. Exploded view of a harmonic drive showing the three components.

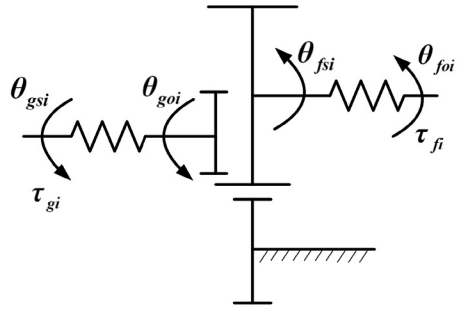

Fig. 2. Kinematic representation of a harmonic drive showing the three ports.

shown in Fig. 1. The wave generator is connected to a motor, the circular spline is connected to the joint base, and the flexspline is sandwiched in between the circular spline and the wave generator and connected to the joint output. The wave generator consists of an elliptical disk, called wave generator plug, and an outer raced ball-bearing assembly. The wave generator plug is inserted into the ball-bearing assembly, thereby giving the bearing an elliptical shape as well. The flexspline is a thin cylindrical cup with external teeth at the open end of the cup having a slightly smaller pitch diameter than the internal teeth of the circular spline. Once assembled, the flexspline fits tightly over the wave generator, therefore, when the wave generator plug is rotated the flexspline deforms and molds into the shape of the rotating ellipse. The circular spline has two more teeth than the flexspline, because of which there exists a small phase difference between the corresponding teeth in engagement [30].

Owing to flexibility of flexspline and wave generator, a kinematic representation of a harmonic drive is illustrated in Fig. 2. Therefore, flexspline and wave generator torsion are defined as follows:

$$\Delta\theta_{fi} = \theta_{foi} - \theta_{fsi}, \tag{1}$$

$$\Delta\theta_{gi} = \theta_{goi} - \theta_{gsi}, \tag{2}$$

where θ_{foi} and θ_{fsi} denotes the flexspline angular position at the load side and gear-side (gear-toothed circumference), respectively. θ_{goi} and θ_{gsi} denote the positions of the wave generator outside part (ball bearing outer rim) and the center part (wave generator plug), respectively.

When the harmonic drive torsion is assumed to be caused by flexspline only, the torsional angle can also be determined as:

$$\Delta\theta_i = \theta_{foi} - \theta_{fsi}. \tag{3}$$

Due to the circular spline is usually fixed leaving the wave generator and flexspline for input and output, $\theta_{ci} = \omega_c i = 0$ and the reaction torque T_{ci} is not of a concern. So the relationship between the positions of the wave generator center part (wave generator plug) and the flexspline angular position at the gear-side (gear-toothed circumference) is given as follows:

$$\theta_{gsi} = -\gamma_i \theta_{fsi}, \tag{4}$$

where γ_i denotes the gear ratio.

Note that, θ_{foi} and θ_{goi} are not available as only θ_{fsi} and θ_{gsi} are measured by the link-side encode and the motor-side encoder, respectively. Thus, the harmonic drive torsion can be obtained by using the following expression:

$$\Delta\theta_i = \theta_{foi} + \frac{\theta_{gsi}}{\gamma_i}. \tag{5}$$

By adding and subtracting the terms θ_{fsi} and θ_{goi} to (5), one obtains:

$$\begin{aligned}\Delta\theta_i &= \theta_{foi} - \theta_{fsi} + \left(\theta_{fsi} + \frac{\theta_{goi}}{\gamma_i}\right) - \left(\frac{\theta_{goi}}{\gamma_i} - \frac{\theta_{gsi}}{\gamma_i}\right) \\ &= \Delta\theta_{fi} - \Delta\theta_{gi}/\gamma_i + \theta_{erri},\end{aligned} \tag{6}$$

where θ_{erri} denotes the kinematic error of harmonic drive transmission. Based on the assumption that there is no relative motion between the wave generator output and the flexspline input, we have $\theta_{erri} = 0$.

The flexspline and wave generator torque can be modeled as:

$$\tau_{fi} = K_{fi}\Delta\theta_{fi}, \tag{7}$$

$$\tau_{gi} = K_{gi}\Delta\theta_{gi}, \tag{8}$$

where K_{fi} and K_{gi} denote the stiffness of flexspline and wave generator, respectively.

Define the local elastic coefficient K_{fL} as:

$$K_{fL} = \frac{d\tau_{fi}}{d\Delta\theta_{fi}} = K_{fo}\left(1 + (C_f\tau_{fi})^2\right), \tag{9}$$

where K_{fo} and C_f are constants to be determined. If $K_{fo} \neq 0$, then the flexspline torsion can be calculated as:

$$\Delta\theta_{fi} = \int_0^{\tau_{fi}} \frac{d\tau_{fi}}{K_{fL}} = \frac{\arctan(C_f\tau_{fi})}{C_f K_{fo}}. \tag{10}$$

Define the local elastic coefficient of wave generator can be modeled as:

$$K_{gL} = K_{go}e^{C_g|\tau_{gi}|}, \tag{11}$$

where K_{go} and C_g are constants to be determined. If $K_{go} \neq 0$, then the wave generator torsional angle can be

calculated using the following relation:

$$\Delta\theta_{gi} = \int_0^{\tau_{gi}} \frac{d\tau_{gi}}{K_{gL}} = \frac{sign(\tau_{gi})}{C_g K_{go}} \left(1 - e^{-C_g|\tau_{gi}|}\right). \quad (12)$$

Finally, the total deformation of the harmonic drive is obtained by substituting the flexspline and wave generator deformation given in (10) and (12) into (6):

$$\Delta\theta_i = \frac{\arctan(C_f\tau_{fi})}{C_f K_{fo}} - \frac{sign(\tau_{gi})}{C_g\gamma_i K_{go}} \left(1 - e^{-C_g|\tau_{gi}|}\right). \quad (13)$$

Then,

$$\tau_{fi} = \frac{1}{C_g}\tan\left(C_f K_{fo}\left(\Delta\theta_i + \frac{sign(\tau_{gi})}{C_g\gamma_i K_{go}}\left(1 - e^{-C_g|\tau_{gi}|}\right)\right)\right), \quad (14)$$

where the wave generator torque τ_{gi} can be approximated by the motor torque command.

By the following formula, one can get the constrained torque, which is obtained by the constrained force on the end-effector of manipulator:

$$\tau_{ci} = \tau_{fie} - \tau_{fio}, \quad (15)$$

where τ_{fio} denotes the joint torque which is obtained in free space, τ_{fie} denotes the total joint torque in the constrained space, which consist of constrained torque τ_{ci} and joint torque in free space τ_{fio}. The total joint torque τ_{fie} and joint torque in free space τ_{fio} is directly obtained from formula (14) under the condition of constrained space and free space, respectively.

3. DYNAMIC MODEL FORMULATION

For a constrained reconfigurable manipulator, the motion of the end-effector is constrained by its task environment. The constraint equation can be described as:

$$\Phi(q) = 0. \quad (16)$$

Under the environment constraint, the dynamic model of reconfigurable manipulator with n-DOF can be described as follows:

$$M(q)\ddot{q} + C(q,\dot{q})\dot{q} + G(q) + F(q,\dot{q}) = u + \tau_c, \quad (17)$$

where $q \in R^n$ is the vector of joint displacements, $M(q) \in R^{n\times n}$ is the symmetric and positive definite inertia matrix, $C(q,\dot{q}) \in R^n$ is the matrix of centripetal Coriolis matrix, $G(q) \in R^n$ is the gravity vector, $u \in R^n$ is the control torque of output side in harmonic drive transmission, $F(q,\dot{q}) \in R^n$ denotes the joint friction force item, $\tau_c \in R^n$ is the constrained torque which obtained by the constrained force on the end-effector of manipulator.

In the multidegree-of-freedom manipulator, the constrained torque vector for all joint τ_c relates to the constrained force on the end-effector of manipulator f as follows:

$$\tau_c = J_\Phi^T(q) f, \quad (18)$$

where $J_\Phi^T(q) \in R^{m\times n}$ is the Jacobian matrix, f denotes the constrained force on the end-effector of manipulator.

Considering each of the joint modules as a subsystem, the dynamics of module i can be expressed as [31]:

$$M_i(q_i)\ddot{q}_i + C_i(q_i,\dot{q}_i)\dot{q}_i + G_i(q_i) + F_i(q_i,\dot{q}_i) + Z_i(q,\dot{q},\ddot{q}) = u_i + \tau_{ci}, \quad (19)$$

with

$$Z_i(q,\dot{q},\ddot{q}) = \left\{\begin{array}{l}\sum_{j=1,j\neq i}^{n} M_{ij}(q)\ddot{q}_j \\ +[M_{ii}(q) - M_i(q_i)]\ddot{q}_i\end{array}\right\} + \left\{\begin{array}{l}\sum_{j=1,j\neq i}^{n} C_{ij}(q,\dot{q})\dot{q}_j \\ +[C_{ii}(q,\dot{q}) - C_i(q_i,\dot{q}_i)]\dot{q}_i\end{array}\right\} + [\bar{G}_i(q) - G_i(q_i)].$$

where q_i, $\dot{q}_i$, $\ddot{q}_i$, $\bar{G}_i(q)$, $F_i(q_i,\dot{q}_i)$, u_i and τ_{ci} are the ith element of the vectors q, $\dot{q}$, $\ddot{q}$, $G(q)$, $F(q,\dot{q})$, u and τ_c, respectively. $M_{ij}(q)$ and $C_{ij}(q,\dot{q})$ are the ijth element of the matrices $M(q)$ and $C(q,\dot{q})$, respectively.

In virtue of there are some unmodelled dynamics in system, the actual parameter of each joint subsystem could be decomposed into nominal part and uncertain part, so Eq. (19) becomes:

$$(M_{i0} + \Delta M_{i0})\ddot{q}_i + (C_{i0} + \Delta C_{i0})\dot{q}_i + G_{i0} + \Delta G_{i0} + F_i(q_i,\dot{q}_i) + Z_i(q,\dot{q},\ddot{q}) = u_i + \tau_{ci}, \quad (20)$$

where M_{i0}, C_{i0}, G_{i0} are the nominal part and the ΔM_{i0}, ΔC_{i0}, ΔG_{i0} are the uncertain part. It is clear that Eq. (20) could be expressed as:

$$M_{i0}\ddot{q}_i + C_{i0}\dot{q}_i + G_{i0} + F_i(q_i,\dot{q}_i) + h_i(q,\dot{q},\ddot{q}) = u_i + \tau_{ci}, \quad (21)$$

where $h_i(q,\dot{q},\ddot{q}) = \Delta M_{i0}\ddot{q}_i + \Delta C_{i0}\dot{q}_i + \Delta G_{i0} + Z_i(q,\dot{q},\ddot{q})$ is the unknown item.

For reconfigurable manipulator system, the parameters of (21) have the following properties [31].

Property 1: Symmetry and boundedness of M_{i0} satisfy the following formula:

$$0 < m_i I \leq M_{i0} \leq \overline{m}_i I, \quad (22)$$

where m_i and $\overline{m}_i$ are unknown positive constants.

Property 2: Boundedness of C_{i0}, for $m_{ci} > 0$:

$$|C_{i0}\dot{q}_i| \leq m_{ci}\dot{q}_i^2, \quad (23)$$

Property 3: Boundedness of G_{i0}, for $m_{gi} > 0$:

$$|G_{i0}| \leq m_{gi}. \quad (24)$$

The constrained reconfigurable manipulator dynamic model of nonlinear interconnected subsystem S_i can be presented by the following state equation:

$$S_i : \left\{\begin{array}{l}\dot{x}_i = A_i x_i + B_i\left[f_i(q_i,\dot{q}_i) + g_i(q_i)(u_i + \tau_{ci}) + h_i(q,\dot{q},\ddot{q})\right], \\ y_i = C_i x_i,\end{array}\right. \quad (25)$$

where $x_i = [x_{i1}, x_{i2}]^T = [q_i, \dot{q}_i]^T, (i = 1,2,...,n)$ is the state vector of subsystem S_i, and y_i is the output of subsystem

S_i. The matrices:

$$A_i = \begin{bmatrix} 0 & 1 \\ 0 & 0 \end{bmatrix} \quad B_i = \begin{bmatrix} 0 \\ 1 \end{bmatrix} \quad C_i = \begin{bmatrix} 1 & 0 \\ 0 & 1 \end{bmatrix},$$
$$f_i(q_i,\dot{q}_i) = M_{i0}^{-1}(q_i) \begin{bmatrix} -C_{i0}(q_i,\dot{q}_i)\dot{q}_i - G_{i0}(q_i) \\ -F_i(q_i,\dot{q}_i) \end{bmatrix},$$
$$g_i(q_i) = M_{i0}^{-1}(q_i),$$
$$h_i(q,\dot{q},\ddot{q}) = -M_{i0}^{-1}(q_i)\left(\Delta M_{i0}\ddot{q}_i + \Delta C_{i0}\dot{q}_i + \Delta G_{i0} + Z_i(q,\dot{q},\ddot{q})\right).$$

The control objective is to design a robust force/position decentralized control scheme for (25) so that the actual position q and force f of the reconfigurable manipulator can follow their desired trajectories under the condition of existing the model uncertainty in the system.

4. CONTROL DESIGN

This section designs the robust dynamic output feedback controller to insure the reconfigurable manipulator system asymptotically stable while satisfying a prescribed H_∞ performance level.

An augmented system consisting of the system (25) and the integral of the tracking error ($e_{ti} = \int y_{id} - y_i$) is defined as follows:

$$\begin{cases} \dot{\bar{x}}_i = \bar{A}_i\bar{x}_i + \bar{B}_i \begin{bmatrix} f_i(q_i,\dot{q}_i) + g_i(q_i)\times \\ (u_i + \tau_{ci}) + h_i(q,\dot{q},\ddot{q}) \end{bmatrix} + R_i y_{id}, \\ \bar{y}_i = \bar{C}_i\bar{x}_i, \end{cases} \tag{26}$$

where

$$\bar{A}_i = \begin{bmatrix} 0 & -C_i \\ 0 & A_i \end{bmatrix}, \bar{x}_i = \begin{bmatrix} e_{ti} \\ x_i \end{bmatrix}, \bar{B}_i = \begin{bmatrix} 0 \\ B_i \end{bmatrix},$$
$$R_i = \begin{bmatrix} I \\ 0 \end{bmatrix}, \bar{C}_i = \begin{bmatrix} I & 0 \\ 0 & C_i \end{bmatrix}.$$

Assumption 1: The kinematic restriction is given as a rigid surface and frictionless and refers to the fact that the end-effector involved has to track a certain prespecified desired position without losing contact with it.

Assumption 2: The reconfigurable manipulator is operated away from any singularity. In this case, the Jacobian $J_\Phi^T(q)$ is of full rank.

Assumption 3: The error between joint constrained torque estimated value and its actual value is small enough so that it can be ignored.

4.1. Adaptive radial basis function (RBF) neural network identification

The terms of $f_i(q_i,\dot{q}_i)$, $g_i(q_i)$ and $h_i(q,\dot{q},\ddot{q})$ are unknown continuous functions because of there are many possible configurations for reconfigurable modular manipulators. To overcome this difficulty, the Radial Basis Function (RBF) neural network, which is proven to be universal approximators of nonlinear input-output relationships with any complexity is employed to approximate the unknown terms. The radial basis function (RBF) network derives from the theory of function approximation. It is a popular alternative to the multilayer perceptron since it has a simpler architecture and a much faster training process. An input layer consisting of sources node; a hidden layer in which each neuron computes its output using a radial basis function, that being in general a Gaussian function, and an output layer that builds a linear weighted sum of hidden neuron outputs and supplies the response of the network.

Assumption 4 [32]**:** Boundedness of the interconnection term, for $d_{ij} \geq 0$, $h_i(q,\dot{q},\ddot{q})$ and $p \geq 1$:

$$\|h_i(q,\dot{q},\ddot{q})\| \leq \sum_{j=1}^{n} d_{ij}Q_j, \tag{27}$$

where $Q_j = 1 + \|q_j\| + \|\dot{q}_j\| + \ldots + \|q_j\|^p + \|\dot{q}_j\|^p$.

For each system, three-layer neural networks are applied to approximate $f_i(q_i,\dot{q}_i)$, $g_i(q_i)$ and $h_i(q,\dot{q},\ddot{q})$, where hidden layer contains seven neurons. The neural network Gaussian basis function is as follows:

$$\Phi_i = \exp\left(-\|X - C_j\|^2 \Big/ 2b_j^2\right), \tag{28}$$

where c_j, b_j, $j = 1,2,\ldots,m$ are the radial basis function neural networks centers and widths respectively.

The RBF neural network expressed as (29) is proposed to compensate the unknown term [33]:

$$h_i(|x_{ie}|, W_{ih}) = W_{ih}^T\Phi_{ih}(|x_{ie}|) + \varepsilon_{ih}, \quad \|\varepsilon_{ih}\| \leq \varepsilon_1, \tag{29}$$

where the W_{ih} is the ideal neural network weights, Φ_{ih} is the neural network basis function, ε_{ih} is the neural network approximation errors, ε_1 is known constant.

Define $\hat{W}_{ih}$ as the estimations of W_{ih}. $\hat{h}_i(|x_{ie}|, \hat{W}_{ih})$ is estimation value of $h_i(|x_{ie}|, W_{ih})$, and can be expressed as:

$$\hat{h}_i(|x_{ie}|, \hat{W}_{ih}) = \hat{W}_{ih}^T\Phi_{ih}(|x_{ie}|). \tag{30}$$

Define the estimation errors as $\tilde{W}_{ih} = W_{ih} - \hat{W}_{ih}$. Therefore,

$$\begin{aligned} h_i(|x_{ie}|, W_{ih}) - \hat{h}_i(|x_{ie}|, \hat{W}_{ih}) \\ = \tilde{W}_{ih}^T\Phi_{ih}(|x_{ie}|) + \varepsilon_{ih}. \end{aligned} \tag{31}$$

According Property1-3, we can obtained that $f_i(q_i,\dot{q}_i)$ and $g_i(q_i)$ are bounded. Similarly, using the RBF neural networks to approximate the nonlinear term $f_i(q_i,\dot{q}_i)$ and $g_i(q_i)$ as follows:

$$f_i(q_i,\dot{q}_i,W_{if}) = W_{if}^T\Phi_{if}(q_i,\dot{q}_i) + \varepsilon_{if} \quad \|\varepsilon_{if}\| \leq \varepsilon_2, \tag{32}$$

$$g_i(q_i,W_{ig}) = W_{ig}^T\Phi_{ig}(q_i) + \varepsilon_{ig} \qquad \|\varepsilon_{ig}\| \leq \varepsilon_3, \tag{33}$$

where the W_{if} and W_{ig} are the ideal neural network weights, $\Phi(\cdot)$ is the neural network basis function, ε_{if} and ε_{ig} are the neural network approximation errors, ε_2, ε_3 are known constants.

Define $\hat{W}_{if}$ and $\hat{W}_{ig}$ as the estimations of W_{if} and W_{ig}, respectively. $\hat{f}_i(q_i,\dot{q}_i,\hat{W}_{if})$ is estimation value of $f_i(q_i,\dot{q}_i,W_{if})$ and $\hat{g}_i(q_i,\hat{W}_{ig})$ is estimation value of $g_i(q_i,W_{ig})$. $\hat{f}_i(q_i,\dot{q}_i,\hat{W}_{if})$ and $\hat{g}_i(q_i,\hat{W}_{ig})$ can be expressed

as:

$$\hat{f}_i\left(q_i,\dot{q}_i,\hat{W}_{if}\right)=\hat{W}_{if}^T\Phi_{if}\left(q_i,\dot{q}_i\right), \tag{34}$$

$$\hat{g}_i\left(q_i,\hat{W}_{ig}\right)=\hat{W}_{ig}^T\Phi_{ig}\left(q_i\right). \tag{35}$$

Define the estimation errors as $\tilde{W}_{if}=W_{if}-\hat{W}_{if}$ and $\tilde{W}_{ig}=W_{ig}-\hat{W}_{ig}$. Therefore,

$$\begin{aligned} &f_i\left(q_i,\dot{q}_i,W_{if}\right)-\hat{f}_i\left(q_i,\dot{q}_i,\hat{W}_{if}\right)\\ &\quad=\tilde{W}_{if}^T\Phi_{if}\left(q_i,\dot{q}_i\right)+\varepsilon_{if}, \end{aligned} \tag{36}$$

$$\begin{aligned} &g_i\left(q_i,W_{ig}\right)-\hat{g}_i\left(q_i,\hat{W}_{ig}\right)\\ &\quad=\tilde{W}_{ig}^T\Phi_{ig}\left(q_i\right)+\varepsilon_{ig}, \end{aligned} \tag{37}$$

Defining approximation error:

$$\omega_{i1}=\varepsilon_{if}+\varepsilon_{ig}\left(u_i+\tau_{ci}\right), \tag{38}$$

$$\omega_{i2}=\varepsilon_{ih}, \tag{39}$$

$$\omega_i=\left|\omega_{i1}\right|+\left|\omega_{i2}\right|. \tag{40}$$

With the adaptive update laws as:

$$\dot{\hat{W}}_{if}=\eta_{if}\left(Y\bar{B}_i\bar{x}_i-N\bar{B}_ix_{ic}\right)\Phi_{if}\left(q_i,\dot{q}_i\right), \tag{41}$$

$$\dot{\hat{W}}_{ig}=\eta_{ig}\left(Y\bar{B}_i\bar{x}_i-N\bar{B}_ix_{ic}\right)\Phi_{ig}\left(q_i\right)\left(u_i+\tau_{ci}\right), \tag{42}$$

$$\dot{\hat{W}}_{ih}=\eta_{ih}\left(Y\bar{B}_i\bar{x}_i-N\bar{B}_ix_{ic}\right)\Phi_{ih}\left(\left|x_{ie}\right|\right), \tag{43}$$

$$\dot{\hat{\omega}}_i=\lambda\left(Y\bar{B}_i\bar{x}_i-N\bar{B}_ix_{ic}\right), \tag{44}$$

where η_{if}, η_{ig}, η_{ih} and λ are positive constants.

4.2. Dynamic output feedback controller design

Considering augmented constrained subsystems Dynamic model (26) , the dynamic output feedback controller is designed as follows:

$$\begin{cases} \dot{x}_{ic}=A_{ic}x_{ic}+B_{ic}\bar{y}_i,\\ u_i=\dfrac{1}{\hat{g}_i\left(q_i,\hat{W}_{ig}\right)}\left[C_{ic}x_{ic}+D_{ic}\bar{y}_i-\hat{f}_i\left(q_i,\dot{q}_i,\hat{W}_{if}\right)\right.\\ \qquad\left.-\hat{h}_i\left(\left|x_{ie}\right|,\hat{W}_{ih}\right)+e_{\tau i}-\hat{\omega}_i\right]-\tau_{ci}, \end{cases} \tag{45}$$

where A_{ic}, B_{ic}, C_{ic} and D_{ic} are the nominal controller gain matrices to be determined. $\hat{\omega}_i$ is used to compensate the influence of control precision due to estimation error of the neural network.

Define the joint torque error as follows:

$$e_{\tau i}=\tau_{ci}-\tau_{di}. \tag{46}$$

Aggregation of (26) and (45) gives the following system:

$$\begin{cases} \dot{x}_{ie}=A_{ie}x_{ie}+B_{ie}d_{ie}+\Delta T_i\\ \bar{y}_{ie}=C_{ie}x_{ie}, \end{cases} \tag{47}$$

where $x_{ie}=\begin{bmatrix}\bar{x}_i\\ x_{ic}\end{bmatrix}$, $A_{ie}=\begin{bmatrix}\bar{A}_i+\bar{B}_iD_{ic}\bar{C}_i & \bar{B}_iC_{ic}\\ B_{ic}\bar{C}_i & A_{ic}\end{bmatrix}$,

$d_{ie}=\begin{bmatrix}e_{\tau i}\\ y_{id}\end{bmatrix}$, $B_{ie}=\begin{bmatrix}\bar{B}_i & R_i\\ 0 & 0\end{bmatrix}$, $C_{ie}=\begin{bmatrix}\bar{C}_i & 0\end{bmatrix}$,

$\Delta T_i=\begin{bmatrix}\bar{B}_i\left[\left(f_i-\hat{f}_i\right)+\left(g_i-\hat{g}_i\right)\left(u_i+\tau_{ci}\right)+h_i-\hat{h}_i-\hat{\omega}_i\right]\\ 0\end{bmatrix}$.

Lemma 1 [34]**:** For any appropriate dimensions constant matrices D, E and any scalar $\varepsilon>0$, the following inequality holds:

$$D^TE+E^TD\le\varepsilon D^TD+\varepsilon^{-1}E^TE. \tag{48}$$

Lemma 2 [35]**:** (Schur Complement Formula) For block matrix $A=\begin{bmatrix}A_{11} & A_{12}\\ A_{12}^T & A_{22}\end{bmatrix}$, the following conditions are proved to be equivalent:

$$(1)A<0, \tag{49}$$

$$(2)A_{11}<0,\quad A_{22}-A_{12}^TA_{11}^{-1}A_{12}<0, \tag{50}$$

$$(3)A_{22}<0,\quad A_{11}-A_{12}A_{22}^{-1}A_{12}^T<0. \tag{51}$$

Lemma 3 [36]**:** In the given system, the eigenvalues of the system are located in a LMI region in the complex plane defined by $D(q,r)$ which is defined by merging different eigenvalues constraints to produce a $D(q,r)$ LMI region in which q and r are the center and radius of the disc region. If there exist symmetric positive-definite matrices X, Y and matrices A_{ic}, B_{ic}, C_{ic}, D_{ic}, as well as the corresponding LMI such that:

$$\begin{bmatrix}X & I\\ I & Y\end{bmatrix}>0, \tag{52}$$

$$\begin{bmatrix} A_{11} & A_{12} & \bar{B}_i & R_i\\ A_{12}^T & A_{22} & Y\bar{B}_i & YR_i\\ * & * & -\gamma_c^2I & 0\\ * & * & * & E^TE-\gamma_c^2I\\ * & * & * & *\\ * & * & * & *\\ * & * & * & * \end{bmatrix}$$

$$\begin{bmatrix} X\bar{C}_i^T & -X\bar{C}_i^T & 0\\ \bar{C}_i^T & -\bar{C}_i^T & 0\\ 0 & 0 & 1\\ 0 & 0 & 0\\ -I & 0 & 0\\ * & -\varepsilon^{-1} & 0\\ * & * & -\varepsilon \end{bmatrix}<0, \tag{53}$$

where

$$A_{11}=\bar{A}_iX+X\bar{A}_i^T+\bar{B}_i\tilde{C}_{ic}+\left(\bar{B}_i\tilde{C}_{ic}\right)^T, \tag{54}$$

$$A_{12}=\tilde{A}_{ic}^T+\bar{A}_i+\bar{B}_i\tilde{D}_{ic}\bar{C}_i, \tag{55}$$

$$A_{22}=Y\bar{A}_i+\bar{A}_i^TY+\tilde{B}_{ic}\bar{C}_i+\left(\tilde{B}_{ic}\bar{C}_i\right)^T, \tag{56}$$

hold, the system is stable and the H_∞ performance is guaranteed with an attenuation level γ.

The controller gains are thus calculated as follows:

$$D_{ic}=\tilde{D}_{ic}, \tag{57}$$

$$C_{ic}=\left(\tilde{C}_{ic}-D_{ic}\bar{C}_iX\right)M^{-T}, \tag{58}$$

$$B_{ic}=N^{-1}\left(\tilde{B}_{ic}-Y\bar{B}_iD_{ic}\right), \tag{59}$$

$$\begin{aligned} A_{ic}=N^{-1}&\left[\tilde{A}_{ic}-Y\left(\bar{A}_i-\bar{B}_iD_{ic}\bar{C}_i\right)X\right.\\ &\left.-Y\bar{B}_iC_{ic}M^T-NB_{ic}\bar{C}_iX\right]M^{-T}, \end{aligned} \tag{60}$$

where M and N satisfy $MN^T=I-XY$.

Theorem 1: On the based of Lemma3, given $\gamma>0$ and

constrained subsystems dynamic model (26), if there exist symmetric positive-definite matrices X, Y and matrices A_{ic}, B_{ic}, C_{ic} and D_{ic}, as well as matrix LMI such that (53) holds, then system (26) is robust asymptotically stable and satisfies the H_∞ performance indicator as follows:

$$\|\dot{e}_{ti}\|^2 \leq \gamma^2 \|d_{ie}\|^2 + V(0), \tag{61}$$

where $\|\dot{e}_{ti}\|^2 = \int_0^{t_1} (\dot{e}_{ti}^T \dot{e}_{ti}) dt$, $\|d_{ie}\|^2 = \int_0^{t_1} ({d_{ie}}^T d_{ie}) dt$.

Proof: Design the Lyapunov function candidate as:

$$V = x_{ie}^T P_1 x_{ie} + \frac{1}{2\eta_{if}} \tilde{W}_{if}^T \tilde{W}_{if} + \frac{1}{2\eta_{ig}} \tilde{W}_{ig}^T \tilde{W}_{ig} + \frac{1}{2\eta_{ih}} \tilde{W}_{ih}^T \tilde{W}_{ih} + \frac{1}{2\lambda} \tilde{\omega}_i^T \tilde{\omega}_i. \tag{62}$$

Combine (47) along with the time derivative of V is given by:

$$\begin{aligned}
\dot{V} =& x_{ie}^T \left(A_{ie}^T P_1 + P_1 A_{ie}\right) x_{ie} + x_{ie}^T P_1 B_{ie} d_{ie} \\
&+ d_{ie}^T B_{ie}^T P_1 x_{ie} + \Delta T_i^T P_1 x_{ie} \\
&+ x_{ie}^T P_1 \Delta T_i - \frac{1}{\eta_{if}} \tilde{W}_{if}^T \dot{\hat{W}}_{if} - \frac{1}{\eta_{ig}} \tilde{W}_{ig}^T \dot{\hat{W}}_{ig} \\
&- \frac{1}{\eta_{ih}} \tilde{W}_{ih}^T \dot{\hat{W}}_{ih} - \frac{1}{\lambda} \tilde{\omega}_i^T \dot{\hat{\omega}}_i.
\end{aligned} \tag{63}$$

Set $P_1 = \begin{bmatrix} Y & N \\ N^T & V \end{bmatrix}$, then

$$\begin{aligned}
\dot{V} =& x_{ie}^T \left(A_{ie}^T P_1 + P_1 A_{ie}\right) x_{ie} + x_{ie}^T P_1 B_{ie} d_{ie} \\
&+ d_{ie}^T B_{ie}^T P_1 x_{ie} + (Y \bar{B}_i \bar{x}_i - N \bar{B}_i x_{ic}) \\
&\times \left[\tilde{W}_{if}^T \Phi_{if}(q_i, \dot{q}_i) + \tilde{W}_{ig}^T \Phi_{ig}(q_i)(u_i + \tau_{ci}) \right. \\
&\left. + \tilde{W}_{ih}^T \Phi_{ih}(|x_{ie}|) + \omega_i - \hat{\omega}_i\right] - \frac{1}{\eta_{if}} \tilde{W}_{if}^T \dot{\hat{W}}_{if} \\
&- \frac{1}{\eta_{ig}} \tilde{W}_{ig}^T \dot{\hat{W}}_{ig} - \frac{1}{\eta_{ih}} \tilde{W}_{ih}^T \dot{\hat{W}}_{ih} - \frac{1}{\lambda} \tilde{\omega}_i^T \dot{\hat{\omega}}_i \\
=& x_{ie}^T \left(A_{ie}^T P_1 + P_1 A_{ie}\right) x_{ie} + x_{ie}^T P_1 B_{ie} d_{ie} \\
&+ d_{ie}^T B_{ie}^T P_1 x_{ie} + \tilde{W}_{if}^T \left[(Y \bar{B}_i \bar{x}_i - N \bar{B}_i x_{ic}) \right. \\
&\left. \times \Phi_{if}(q_i, \dot{q}_i) - \eta_{if}^{-1} \dot{\hat{W}}_{if}\right] + \tilde{W}_{ig}^T \left[(Y \bar{B}_i \bar{x}_i \right. \\
&\left. - N \bar{B}_i x_{ic}) \Phi_{ig}(q_i)(u_i + \tau_{ci}) - \eta_{ig}^{-1} \dot{\hat{W}}_{ig}\right] \\
&+ \tilde{W}_{ih}^T \left[(Y \bar{B}_i \bar{x}_i - N \bar{B}_i x_{ic}) \Phi_{ih}(x_{ie}) - \eta_{ih}^{-1} \dot{\hat{W}}_{ih}\right] \\
&+ (Y \bar{B}_i \bar{x}_i - N \bar{B}_i x_{ic})(\omega_i - \hat{\omega}_i) - \frac{1}{\lambda} \tilde{\omega}_i^T \dot{\hat{\omega}}_i.
\end{aligned} \tag{64}$$

Substituting (41)-(43) into (64), we obtain:

$$\begin{aligned}
\dot{V} =& x_{ie}^T \left(A_{ie}^T P_1 + P_1 A_{ie}\right) x_{ie} + x_{ie}^T P_1 B_{ie} d_{ie} + d_{ie}^T B_{ie}^T P_1 x_{ie} \\
&+ (Y \bar{B}_i \bar{x}_i - N \bar{B}_i x_{ic})(\omega_i - \hat{\omega}_i) - \frac{1}{\lambda} \tilde{\omega}_i^T \dot{\hat{\omega}}_i \\
=& x_{ie}^T \left(A_{ie}^T P_1 + P_1 A_{ie}\right) x_{ie} + x_{ie}^T P_1 B_{ie} d_{ie} + d_{ie}^T B_{ie}^T P_1 x_{ie} \\
&+ (Y \bar{B}_i \bar{x}_i - N \bar{B}_i x_{ic}) \tilde{\omega}_i - \frac{1}{\lambda} \tilde{\omega}_i^T \dot{\hat{\omega}}_i \\
=& x_{ie}^T \left(A_{ie}^T P_1 + P_1 A_{ie}\right) x_{ie} + x_{ie}^T P_1 B_{ie} d_{ie} \\
&+ d_{ie}^T B_{ie}^T P_1 x_{ie} + \tilde{\omega}_i \left(Y \bar{B}_i \bar{x}_i - N \bar{B}_i x_{ic} - \frac{1}{\lambda} \dot{\hat{\omega}}_i\right).
\end{aligned} \tag{65}$$

Substituting (44) into (65) yields:

$$\begin{aligned}
\dot{V} =& x_{ie}^T \left(A_{ie}^T P_1 + P_1 A_{ie}\right) x_{ie} + x_{ie}^T P_1 B_{ie} d_{ie} \\
&+ d_{ie}^T B_{ie}^T P_1 x_{ie}.
\end{aligned} \tag{66}$$

Given the following index:

$$J = \int_0^{t_1} (\dot{e}_{ti}^T \dot{e}_{ti} - \gamma^2 d_{ie}^T d_{ie}) dt$$

Thus,

$$\begin{aligned}
J &= \int_0^{t_1} (\dot{e}_{ti}^T \dot{e}_{ti} - \gamma^2 d_{ie}^T d_{ie} + \dot{V}) dt - \int_0^{t_1} \dot{V} dt \\
&= \int_0^{t_1} (\dot{e}_{ti}^T \dot{e}_{ti} - \gamma^2 d_{ie}^T d_{ie} + \dot{V}) dt - V(t_1) + V(0) \\
&\leq \int_0^{t_1} (\dot{e}_{ti}^T \dot{e}_{ti} - \gamma^2 d_{ie}^T d_{ie} + \dot{V}) dt + V(0),
\end{aligned} \tag{67}$$

where

$$\begin{aligned}
\dot{e}_{ti}^T \dot{e}_{ti} &= (y_{id} - \bar{y}_i)^T (y_{id} - \bar{y}_i) \\
&= y_{id}^T y_{id} - \bar{y}_i^T y_{id} - y_{id}^T \bar{y}_i + \bar{y}_i^T \bar{y}_i.
\end{aligned}$$

Let $E = \begin{bmatrix} 0 & I \end{bmatrix}$, one can obtain:

$$\begin{aligned}
\dot{e}_{ti}^T \dot{e}_{ti} =& d_{ie}^T E^T E d_{ie} - d_{ie}^T E^T C_{ie} x_{ie} \\
&- x_{ie}^T C_{ie}^T E d_{ie} + x_{ie}^T C_{ie}^T C_{ie} x_{ie}.
\end{aligned} \tag{68}$$

Based on (67), for achieve the required performance (61) and stability of the augmented system (45) the following inequality should hold:

$$\dot{V} + \dot{e}_{ti}^T \dot{e}_{ti} - \gamma^2 d_{ie}^T d_{ie} < 0. \tag{69}$$

By using (66), (68) and based on Lemma2, inequality (69) implies that the following inequality must hold:

$$\begin{bmatrix} A_{ie}^T P_1 + P_1 A_{ie} & P_1 B_{ie} - C_{ie}^T E & C_{ie}^T \\ * & E^T E - \gamma^2 I & 0 \\ * & * & -I \end{bmatrix} < 0. \tag{70}$$

Inequality (70) can further decomposed as below:

$$\begin{aligned}
&\begin{bmatrix} A_{ie}^T P_1 + P_1 A_{ie} & P_1 B_{ie} & C_{ie}^T \\ * & E^T E - \gamma^2 I & 0 \\ * & * & -I \end{bmatrix} \\
&+ \begin{bmatrix} -C_{ie}^T \\ 0 \\ 0 \end{bmatrix} \begin{bmatrix} 0 & E & 0 \end{bmatrix} \\
&+ \begin{bmatrix} 0 \\ E \\ 0 \end{bmatrix} \begin{bmatrix} -C_{ie}^T & 0 & 0 \end{bmatrix} < 0.
\end{aligned} \tag{71}$$

Based on Lemma3, inequality (71) is implied by the following inequality:

$$\begin{bmatrix} A_{ie}^T P_1 + P_1 A_{ie} & P_1 B_{ie} \\ * & E^T E - \gamma^2 I \\ * & * \\ * & * \\ * & * \end{bmatrix}$$

(a) (b)

Fig. 3. Configurations for simulation (a) configuration a (b) configuration b.

$$\begin{bmatrix} C_{ie}^T & -C_{ie}^T & 0 \\ 0 & 0 & E \\ -I & 0 & 0 \\ * & -\varepsilon^{-1} & 0 \\ * & * & -\varepsilon \end{bmatrix} < 0. \tag{72}$$

Set

$$F_1 = \begin{bmatrix} X & I \\ M^T & 0 \end{bmatrix}, F_2 = \begin{bmatrix} I & Y \\ 0 & N^T \end{bmatrix},$$

then, it is clear to see that $F_1^T P_1 = F_2^T$.

Pre- and post-multiplying inequality (72) by $\begin{bmatrix} F_1^T & I & I & I & I \end{bmatrix}$ and its transpose respectively, yields:

$$\begin{bmatrix} F_1^T A_{ie}^T F_2 + F_2^T A_{ie} F_1 & F_2^T B_{ie} \\ * & E^T E - \gamma^2 I \\ * & * \\ * & * \\ * & * \\ F_1^T C_{ie}^T & -F_1^T C_{ie}^T & 0 \\ 0 & 0 & E \\ -I & 0 & 0 \\ * & -\varepsilon^{-1} & 0 \\ * & * & -\varepsilon^{-1} \end{bmatrix} < 0. \tag{73}$$

According to (57)-(60), it follows that (73) implies (53). Therefore, the system satisfies the H_∞ performance indicator and this completes the proof of Theorem. □

5. SIMULATION RESULTS

To verify the effectiveness of the proposed dynamic output feedback control strategy, in this subsection, two 2-DOF constrained reconfigurable manipulators with different configurations shown in Fig. 3 are employed for simulation. For the sake of the facilitation of the analysis of the configurations above, we can transform them into a form of analytic charts, which are shown in Fig. 4. The initial position and velocity are set as $q_1(0) = q_2(0) = 1$ and $\dot{q}_1(0) = \dot{q}_2(0) = 0$, respectively. In the examples, the end effectors of the manipulator move along the constraint surface and exert a force on it at the same time. Suppose that there is no Coulomb friction between the end-effector and the contact surface.

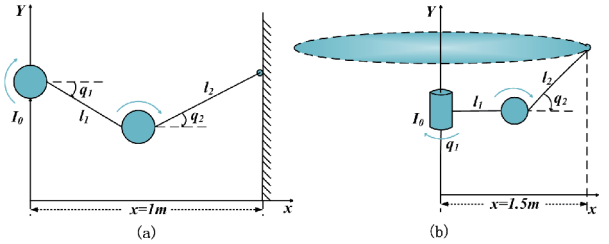

Fig. 4. The analytic charts of the configurations (c) configuration a (d) configuration b.

By using YALMIP Toolbox [37] and selecting LMILab solver under the Matlab software, we can obtain the controller gain matrices listed below:

$$A_{1c} = A_{2c} = \begin{bmatrix} -9.8049 & -16.3541 \\ -0.3971 & -1.0241 \\ -0.1960 & 0 \\ -0.2849 & 0 \end{bmatrix}$$

$$\begin{bmatrix} -0.8216 & -8.4173 \\ 0 & 0 \\ -8.6338 & -1.0073 \\ -1.2445 & -8.6542 \end{bmatrix},$$

$$B_{1c} = B_{2c} = \begin{bmatrix} -2.0415 & 2.9319 \\ 3.0141 & -2.0195 \\ 0.8217 & -0.6597 \\ 2.5280 & 0.0851 \end{bmatrix}$$

$$\begin{bmatrix} 1.0163 & 3.0310 \\ -1.9793 & 3.1419 \\ -1.0068 & -0.2360 \\ -4.2945 & -8.2307 \end{bmatrix},$$

$$C_{1c} = C_{2c} = \begin{bmatrix} -0.3520 & 0.3230 \\ -0.2141 & -0.0560 \end{bmatrix},$$

$$D_{1c} = D_{2c} = \begin{bmatrix} 1.0483 & 1.0481 \\ -1.0523 & -344.30 \end{bmatrix}.$$

Here, the control law (45) is applied to the whole control system, and the control parameters are selected as $\eta_{if} = 0.002$, $\eta_{ig} = 0.002$, $\eta_{ih} = 500$, $\lambda = 0.002$ and the H_∞ performance indicators is defined as $\gamma = 1.0$.

Considering configuration a, the constrained equation can be expressed as:

$$\phi(q) = l_1 \cos(q_1) + l_2 \cos(q_2) - 1 = 0, \tag{74}$$

where l_1, l_2 are the lengths of the two manipulator links. The desired position and the desired constraint force are defined as:

$$q_{1d} = 0.5\cos(t) + 0.3\sin(t), \tag{75}$$

$$q_{2d} = \arccos\left(\frac{1 - l_1 \cos(q_{1d})}{l_2}\right), \tag{76}$$

$$f_d = 10\sin(t)N. \tag{77}$$

Figs. 5 and 6 show that the actual trajectories and the

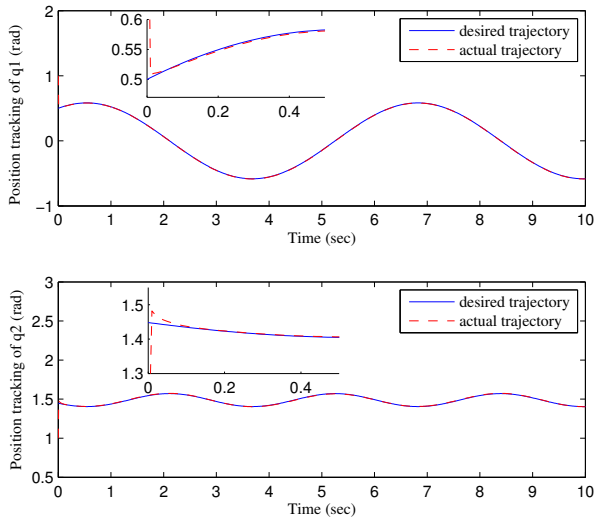

Fig. 5. Position tracking performance of configuration a.

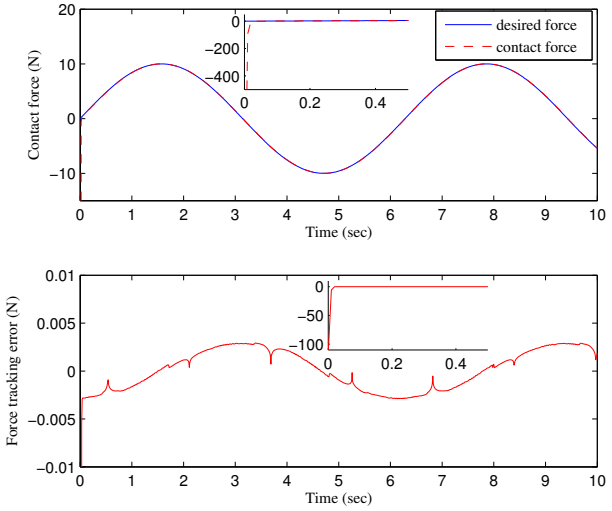

Fig. 7. Force tracking curves and force tracking error of configuration a.

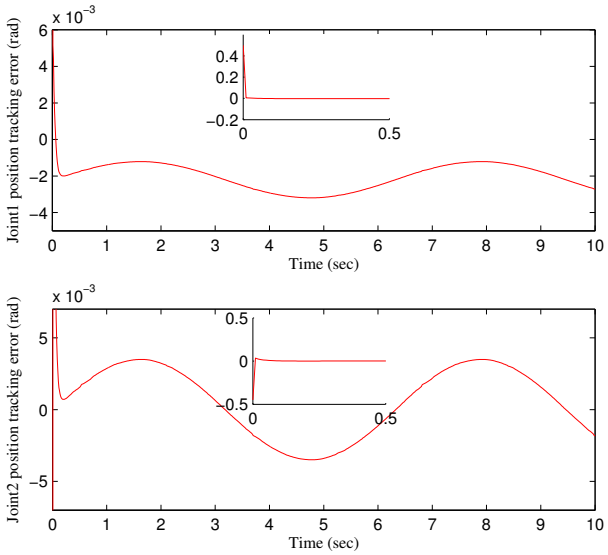

Fig. 6. Position tracking error of configuration a.

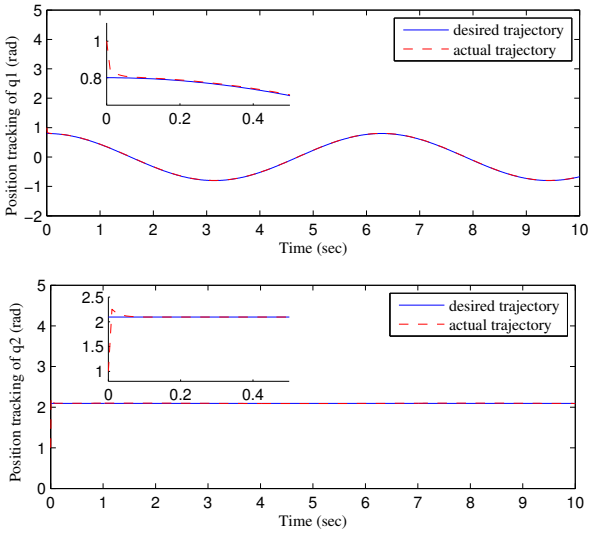

Fig. 8. Position tracking performance of configuration b.

desired trajectories of configuration a are almost overlap. The tracking performance of the contact force and the force tracking error curves is illustrated in Fig. 7, it is clear that the system converges to an error that can be considered as zero. (less than 0.01 N). Given the above, it can be concluded that high performance of the simultaneous force-position tracking is achieved with relatively smooth control effort. The control laws with respect to position and contact force ensures the stable desired position tracking and the desired contact force tracking along the surface normal vector.

In order to further test the effectiveness of the proposed scheme, configuration b is also employed for the simulation. For configuration b, choose a circular path as the environmental constraint, which assumes that the reconfigurable manipulator works in some special occasions such as barrels or cylinders. The constraint equation can be described as $\phi(q) = l_1 + l_2\cos(q_2) - 1.5 = 0$. The desired position and the desired constraint force are defined as:

$$q_{1d} = 0.8\cos(t), \tag{78}$$

$$q_{2d} = \frac{2\pi}{3}, \tag{79}$$

$$f_d = 5N. \tag{80}$$

The parameters of the force/position decentralized controller in configuration b are all chosen the same as those in configuration a . The position tracking performance and force tracking performance of configuration b are shown in Figs. 8- 10, respectively. The simulation results demon-

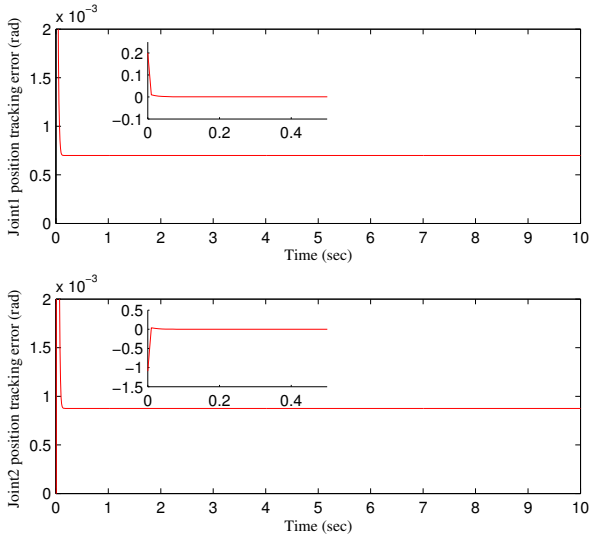

Fig. 9. Position tracking error of configuration b.

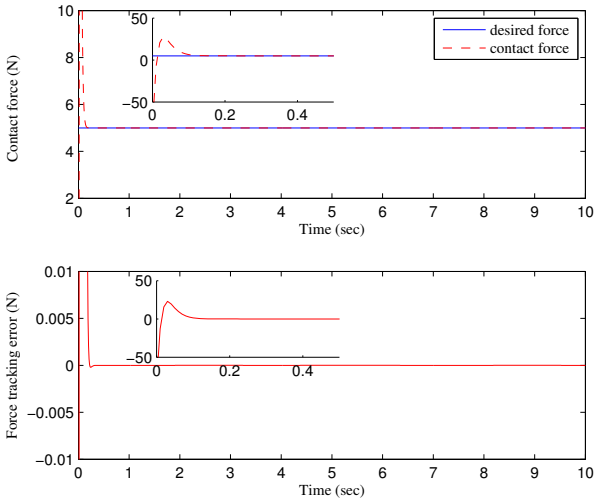

Fig. 10. Force tracking curves and force tracking error of configuration b.

strate that the proposed force/position decentralized control strategy is applicable to different configurations of constrained reconfigurable manipulator without changing any control parameters. This is an important and meaningful advantage for control of reconfigurable manipulator to complete different kinds of tasks in different environment with a requirement of frequent conversion from one configuration to another. It is worth mentioning that the proposed control strategy can also be applied to reconfigurable manipulator with more degrees of freedoms.

To illustrate more on performance of the proposed controller, a comparative study with a fully adaptive neural network controller is done. The fully adaptive neural network control input is given as [38] where a hybrid position/force controller that combines decentralized control with centralized control scheme is designed to control the position and force of the constrained reconfigurable manipulator. Compare with Figs.3-7 as shown in [38], this paper realizes force decentralized control, and reduces the training time of neural network. In addition, the tracking performance of system is approved and the tracking error curve is offered, which makes the tracking performance of the constrained reconfigurable manipulator system expressed more clearly.

6. CONCLUSION

A torque sensorless force/position decentralized robust control is presented for constrained reconfigurable manipulator system. Torque estimation based on position measurements provides an advantage of noise immunity to the estimated joint torque and reduces the cost of joint torque sensing. The radial basis function (RBF) neural network is introduced to approximate the unmodeled dynamics and unknown terms of constrained reconfigurable manipulator subsystem by using adaptive algorithm, simultaneously. Subsequently, the dynamic output feedback controller is designed to realize force/position control and based on Lyapunov theory, the sufficient condition for ensures the reconfigurable manipulator system asymptotically stable while satisfying a prescribed H_∞ performance level is offered in terms of linear matrix inequality (LMI). Finally, the effectiveness of the proposed scheme is verified under the conditions of different configurations without modifying any parameters.

REFERENCES

[1] D. Schmitz, P. Khosla, and T. Kanade, "The CMU reconfigurable modular manipulator system," *Robotics Institute, Carnegie Mellon University, Pittsburgh, PA, Technical Report, CMU-RI-TR-88-07*, 1988.

[2] M. Biglarbegian, W. Melek, and J.M. Mendel, "Design of novel interval type-2 fuzzy controllers for modular and reconfigurable robots: theory and experiments," *IEEE Transactions on Industrial Electronics*, vol. 58, no. 4, pp. 1371-1384, 2011. [click]

[3] T. Sun, Y. Song, Y. LI, and J. Zhang, "Workspace decomposition based dimensional synthesis of a novel hybrid reconfigurable robot," *Journal of Mechanisms and Robotics*, vol. 2, no. 2, pp. 191-220, 2010.

[4] M. R. Faieghi, H. Delavari, and D. Baleanu, "A novel adaptive controller for two-degree of freedom polar robot with unknown perturbations," *Communications in Nonlinear Science and Numerical Simulation*, vol. 17, no. 2, pp. 1021-1030, 2012. [click]

[5] G. Leeena and G. Ray, "A set of decentralized PID controllers for an n-link robot manipulator," *Sadhana*, vol. 37, no. 3, pp. 405-423, 2012.

[6] Y. Yang, C. Hua, and X. Guan, "Adaptive fuzzy synchronization control for networked teleoperation system with input and multi-state constraints," *Journal of the Franklin Institute*, vol. 353, no. 12, pp. 2814-2834, 2016. [click]

[7] C. Hua, G. Liu, L. Zhang, and X. Guan, "Output feedback tracking control for nonlinear time-delay systems with tracking errors and input constraints," *Neurocomputing*, vol. 173, pp. 751-758, 2016. [click]

[8] G. S. Soh and F. Ying, "Motion generation of planar six and eight-bar slider mechanisms as constrained robotic systems," *Journal of Mechanisms and Robotics*, vol. 7, no. 3, 2015.

[9] Z. Li, X. Cao, Y. Tang, R. Li, and W. Ye, "Bilateral teleoperation of holonomic constrained robotic systems with time-varying delays," *IEEE Transactions on Instrumentation and Measure*, vol. 62, no. 4, pp. 752-765, 2013. [click]

[10] S. Bellakehal, N. Andreff, Y. Mezouar, and M. Tadjine, "Vision/force control of parallel robots," *Mechanism and Machine Theory*, vol. 46, no. 10, pp.1376-1395, 2011. [click]

[11] Y. Karayiannidis and Z. Doulgeri, "Robot contact tasks in the presence of control target distortions," *Robotics and Autonomous Systems*, vol. 58, no. 5, pp. 596-606, 2010. [click]

[12] D. Q. Truong and K. K. Ahn, "Force control for press machines using an online smart tuning fuzzy PID based on a robust extended Kalman filter," *Expert Systems with Applications*, vol. 38, no. 5, pp. 5879-5894, 2011.

[13] H. R. Koofigar, "Adaptive tracking with external force disturbance rejection for uncertain Robotic systems," *International Journal of Control, Automation and Systems*, vol. 12, no.1, pp. 169-176, 2014. [click]

[14] S. Ahmad, H. W. Zhang, and G. J. Liu, "Distributed fault detection for modular and reconfigurable robots with joint torque sensing: A prediction error based approach" *Mechatronics*, vol. 23, no.6, pp. 607-616, 2013. [click]

[15] M. Fumagalli, S. Ivaldi, M. Randazzo, L. Natale, G. Metta, G. Sandini, and F. Nori, "Force feedback exploiting tactile and proximal force/torque sensing," *Autonomous Robots*, vol. 33, no.4, pp. 381-398, 2012. [click]

[16] F. Aghili and M. Namvar, "Adaptive control of manipulators using uncalibrated joint-torque sensing," *IEEE Transactions on Robotics*, vol. 22, no.4, pp. 854-860, 2006. [click]

[17] S. Islam and P. X. Liu, "PD output feedback control design for industrial robotic manipulators," *Mechatronics IEEE/ASME Transactions on*, vol. 16, no. 1, pp. 187-197, 2011. [click]

[18] J. W. Grizzle, C. Chevallereau, A. D. Ames, and R.W. Sinnet, "3D bipedal robotic walking: models, feedback control, and open problems," *Automatica*, vol. 50, no. 8, pp. 505-532, 2015.

[19] Y. Hu, G. Yan, and Z. Lin, "Feedback control of planar biped robot with regulable step length and walking speed," *IEEE Transactions on Robotics*, vol. 27, no. 1, pp.162-169, 2011.

[20] S. Dharani, R. Rakkaiyappan, and J. Cao, "Robust stochastic sampled-data H_∞ control for a class of mechanical systems with uncertainties," *ASME Journal of Dynamic Systems, Measurement and Control*, vol. 137, no. 10, pp. 101008-1-101008-14, 2015.

[21] X. M. Zhang and Q. L. Han, "Event-triggered dynamic output feedback control for networked control systems," *Iet Control Theory and Applications*, vol. 8, no. 4, pp. 226-234, 2014. [click]

[22] T. B. Wang, C. D. Wu, Y. L. Wang, and Y. Z. Zhang, "Dynamic output feedback H_∞ control for continuous-time networked control systems," *Control Theory and Applications*, vol. 7, no. 5, pp. 1005-1013, 2013.

[23] M. Sami and R. J. Patton, "Active fault tolerant control for nonlinear systems with simultaneous actuator and sensor faults," *International Journal of Control, Automation and Systems*, vol. 11, no. 6, pp. 1149-1161, 2013. [click]

[24] B. Ranjbar-Sahraei, F. Shabaninia, A. Nemati, and S. Stan, "A novel robust decentralized adaptive fuzzy control for swarm formation of multiagent systems," *IEEE Transactions on Industrial Electronics*, vol. 59, no. 8, pp. 3124-3134, 2012. [click]

[25] Y. Gu, X. Xiang, W. Li, and X. He, " Mode-adaptive decentralized control for renewable DC microgrid with enhanced reliability and flexibility," *IEEE Transactions on Power Electronics*, vol. 29, no. 9, pp. 5072-5080, 2014.

[26] S. Tong, C. Liu, and Y. Li, "Fuzzy-adaptive decentralized output-feedback control for large-scale nonlinear systems with dynamical uncertainties," *IEEE Transactions on Fuzzy Systems*, vol. 18, no. 5, pp. 845-861, 2010. [click]

[27] S. N. Jin, G. H. Lee, and S. Jung, "Position control of a mobile inverted pendulum system using radial basis function network," *International Journal of Control, Automation, and Systems*, vol. 8, no. 1, pp. 157-162, 2010. [click]

[28] H. Yu, T. Xie, S. Paszczynski, and B. M. Wilamowski, "Advantages of radial basis function networks for dynamic system design," *IEEE Transactions on Industrial Electronics*, vol. 58, no. 12, pp. 5438-5450, 2011. [click]

[29] A. Golbabai and H. Rabiei, "Hybrid shape parameter strategy for the RBF approximation of vibrating systems," *International Journal of Computer Mathematics*, vol. 89, no. 17, pp. 1-18, 2012.

[30] H. Zhang, S. Ahmad, and G. Liu, "Modeling of torsional compliance and hysteresis behaviors in harmonic drives," *IEEE/ASME Transactions on Mechatronics*, vol. 20, no. 1, pp. 178-185, 2015. [click]

[31] M. Zhu and Y. LI, "Decentralized adaptive fuzzy sliding mode control for reconfigurable modular manipulators," *International Journal of Robust and Nonlinear Control*, vol. 20, no. 4, pp. 472-488, 2010.

[32] Y. Tang, M. Tomizuka, and G. Guerrero, "Decentralized robust control of mechanical systems," *IEEE Transactions on Automatic Control*, vol. 45, no. 4, pp. 771-775, 2000.

[33] B. Zhao and Y. Li, "Local joint information based active fault tolerant control for reconfigurable manipulator," *Nonlinear Dynamics*, vol. 77, no. 3, pp. 859-876, 2014. [click]

[34] X. LI and C. E. D. Souza, " Delay-dependent robust stability and stabilization of uncertain linear delay systems: a linear matrix inequality approach," *IEEE Trans. Automat. Cont.*, vol. 42, no. 9, pp. 1144-1148, 1997.

[35] L. S. Bai, Z. H. Tian, and S. J. Shi, "Robust fault detection for a class of nonlinear time-delay system," *Journal of the Franklin Institute*, vol. 344, no. 6, pp. 873-888, 2007.

[36] M. Sami and R. J. Patton, "Active fault tolerant control for nonlinear systems with simultaneous actuator and sensor faults," *International Journal of Control, Automation and Systems*, vol. 11, no. 6, pp. 1149-1161, 2013. [click]

[37] J. Lofberg, "A toolbox for modeling and optimization in MATLAB," *Optimization*, pp. 284-289, 2004. [click]

[38] Y. Li, G. Wang, B. Dong, and B. Zhao, "Hybrid position-force control for constrained reconfigurable manipulators based on adaptive neural network," *Advances in Mechanical Engineering*, vol. 7, no. 9, pp. 364-383, 2015.

Fan Zhou received her B.S. and M.S. degrees from Changchun University of Technology, China, in 2012 and 2015, respectively. She is currently working towards a Ph.D. degree in the Department of Control Engineering, Changchun University of Technology, China. Her research interests include intelligent mechanical, robot control, and robust control.

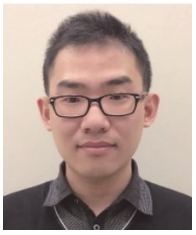

Bo Dong received his M.S. and Ph.D degrees from Jilin University, China in 2012 and 2015, respectively. He is currently a postdoctoral fellow in State Key Laboratory of Management and Control for Complex Systems, Institute of Automation, Chinese Academy of Sciences, Beijing, China. His research interests include intelligent mechanical and robot control.

Yuanchun Li received his M.S. and Ph.D degrees from Harbin Institute of Technology, China in 1987 and 1990, respectively. He is currently a Professor in Changchun University of Technology, China. He is also a Professor in Jilin University, China. His research interest covers complex system modeling, intelligent mechanical, and robot control.